Information-theoretic approach to high-temperature spin dynamics

P. A. Fedders and A. E. Carlsson
Department of Physics, Washington University, Saint Louis, Missouri 63130
(Received 19 February 1985)

The information-theoretic maximum-entropy approach is used to obtain high-temperature dynamical spin-correlation functions from a finite number of rigorously known moments. The method is applied to the dipolar-broadened magnetic-resonance line-shape function for a simple cubic lattice and other spin-correlation functions. The results improve on the best previous theoretical results and agree with experiment to within $\sim 2\%$. Modeling of the self-energy with the maximum-entropy method provides better results than direct modeling of the line-shape function. The results display an oscillating pattern of convergence which is expected to occur in many physical applications.

I. INTRODUCTION

Information theory or the maximum-entropy (ME) approach has been used lately to obtain solutions to several types of undetermined inverse problems.[1] In particular, a ME technique has recently been developed[2] for obtaining a spectral function given a finite number of its moments. In this paper we use the ME approach to obtain the dynamical correlation functions for high-temperature spin systems from a finite number of known moments.

We consider two specific spin-correlation functions:

(1) The dipolar-broadened magnetic-resonance line-shape function for a simple-cubic lattice of spin-$\frac{1}{2}$ nucleons. This is the classic spin line-shape problem and attempts have been made at fitting or calculating the function for almost thirty years.[3] Other than its age and venerability, this function is a good choice for a test case because the function is accurately known over a reasonable large time domain from free-induction-decay experiments.[4] Further, the first eight moments have been calculated.[5]

(2) The spectral function in the q-independent bubble approximation for the Heisenberg paramagnet.[6] This function is not physically measurable, but it is the solution to a one-dimensional integral equation and can thus be obtained to arbitrary accuracy. In addition, any finite number of its moments can be calculated with little computational effort.

This paper also discusses two points regarding the application of ME to spin problems such as these. First, dynamical spin-correlation functions do not possess a cutoff in frequency space but die off exponentially instead. Our results and arguments indicate that this affects the convergence of the sequence of ME approximations. Second, we find that a more accurate solution is generally obtained by fitting the self-energy associated with a spin-correlation function than by fitting the spin-correlation function itself.

As mentioned earlier, there have been numerous attempts at fitting dynamical spin-correlation functions by matching parameters in an assumed functional form to a finite number of moments. We shall not comment on these except to note that given the answer one wants, one can almost always invent an appropriate analytic functional form. The ME method, on the other hand, provides a specific functional form based on an "unbiased" guess for the values of the unknown moments, which can, in principle, be carried to arbitrarily high orders. Thus the method describes a sequence of approximations whose convergence can be systematically analyzed.

In the rest of this section we shall introduce definitions and notation that are used in the rest of the paper. Section II contains a description of the calculations and their results, while Sec. III contains a summary and a discussion of these results.

We define a time-dependent spin-correlation function as

$$G(t)=\langle I_x(t)I_x(0)\rangle\Theta(t)/\langle I_x^2\rangle \ , \tag{1}$$

where $I_x(t)$ is a nuclear-spin operator in the Heisenberg representation, the angular brackets $\langle A\rangle$ denote the thermal average of A, and $\Theta(t)$ is the step function. The correlation function in frequency space, $G(\omega)$, is defined as

$$G(\omega)=\int_{-\infty}^{\infty} dt\, G(t)e^{i\omega t} \ . \tag{2}$$

It is also convenient to define a self-energy $\Sigma(\omega)$ by the equation

$$[\omega-\Sigma(\omega)]G(\omega)=i \ . \tag{3}$$

As will be discussed in Sec. II, the analysis of the properties of G is simplified by a consideration of Σ.[6] Both $G(\omega)$ and $\Sigma(\omega)$ are complex quantities and are conveniently described by their spectral functions $A(\omega)$ and $\Gamma(\omega)$, where

$$A(\omega)=\mathrm{Re}G(\omega) \ , \quad \Gamma(\omega)=-\mathrm{Im}\Sigma(\omega) \ . \tag{4}$$

For example,[5] the moments of G and Σ are usually defined as

$$M_n=\int_{-\infty}^{\infty}\frac{d\omega}{\pi}\omega^n A(\omega) \ , \quad n\geq 0$$
$$L_n=\int_{-\infty}^{\infty}\frac{d\omega}{\pi}\omega^{n-2}\Gamma(\omega) \ , \quad n\geq 2 \tag{5}$$

where $M_0=1$, and M_n and L_n both have the units of ω^n. These moments are related to each other by the equation

$$M_{n+1}=\sum_{k=1}^{n+1} L_k M_{n+1-k} \ . \tag{6}$$

In the problems considered in this paper, only the even moments are nonzero.

II. CALCULATIONS AND RESULTS

In this section we describe the ME calculations that were mentioned in Sec. I. Both $\Gamma(\omega)$ and $A(\omega)$ will be expanded as

$$P_N(\omega)=Z^{-1}\exp\left[-\sum_{n=1}^{N}\lambda_n\omega^n\right] . \tag{7}$$

Only the even λ_n are nonzero and the N values λ_n are determined by the first N moments. The numerical calculations were carried out as described in Ref. 2. By a "converged calculation" we mean that the λ_n are independent of the size of the frequency interval used to calculate the moments, as the interval becomes infinite. By a nonconverged calculation we mean that the λ_n depend on the size of the frequency interval used even as the interval approaches infinity. The fit in the latter case, of course, has no meaning. Finally, in both examples in this section, we will use dimensionless units where all frequencies are expressed in terms of $(M_2)^{1/2}$. We shall denote the moments in these reduced units as m_n and l_n, where

$$\begin{aligned} m_n &= M_n/(M_2)^{n/2} \ , \\ l_n &= L_n/(M_2)^{n/2} \ . \end{aligned} \tag{8}$$

A. Dipolar linewidth

The reduced moments up to m_8 and l_8 calculated from Ref. 5 for magnetic fields along the three common crystallographic directions are displayed in Table I. These are then used in conjunction with Eq. (7) and the procedure described in Ref. 2 to obtain the λ_n and Z. In fact, the ME procedure has already been applied to this function,[7,8] but only including m_2 and m_4.

We have calculated $A_N(\omega)$, where

TABLE I. Reduced moments of the dipolar line-shape function (Ref. 4) for three crystal directions of the magnetic field.

	Crystal direction		
	[100]	[110]	[111]
m_2	1	1	1
m_4	2.1244	2.3019	2.3690
m_6	6.2228	7.4791	8.0438
m_8	24.5798	33.5277	40.8099
l_2	1	1	1
l_4	1.1244	1.3019	1.3690
l_6	2.9740	3.8753	4.3059
l_8	12.994	19.176	25.217

TABLE II. Values of the λ_n for $A_8(\omega)$.

	Crystallographic direction		
	[100]	[110]	[111]
Z	3.2826	2.9766	2.8990
λ_2	-0.16022	0.10625	0.17105
λ_4	0.18490	0.91238×10^{-1}	0.73681×10^{-1}
λ_6	-0.70911×10^{-2}	-0.11952×10^{-2}	-0.85184×10^{-3}
λ_8	0.71366×10^{-4}	0.39155×10^{-5}	0.24480×10^{-5}

$$A_N(\omega)=Z^{-1}\exp\left[-\sum_{n=1}^{N}\lambda_n\omega^n\right] \tag{9}$$

for $N=2,4,6,8$ for all three crystallographic directions. We find that the calculation converges for $N=2$, 4, and 8, but not for $N=6$. For reasons to be discussed latter, we believe that values of $N=4k+2$, where k is a positive integer, lead to nonconvergent calculations. The Z's and λ_n's obtained for $N=8$ are given in Table II. We have also calculated $\Gamma_N(\omega)$, where

$$\Gamma_N(\omega)=Z^{-1}\exp\left[-\sum_{n=1}^{N}\lambda_n\omega^n\right] \tag{10}$$

for $N=2$, 4, and 6 for all crystallographic directions. We note that Γ_N requires the moments up to M_{N+2}. In this case the calculation converges for $N=2$ and 4, but not for $N=6$. Again, we believe that values $N=4k+2$ will not converge. The calculated values of the λ_n are displayed in Table III.

Figure 1 shows the experimental line-shape function[4] for a magnetic field along the [110] direction, along with two theoretical curves: the eight-moment ME approximation $a_8(\omega)$, and the line-shape function obtained from the four-moment ME approximation $\Gamma_4(\omega)$ to the self-energy [which produces *six* correct moments of $A(\omega)$]. The two theoretical curves agree roughly equally well with experiment. For small ω, both are within 2% of the experimental curve. For large ω the tail of the experimental curve lies below both of the theoretical curves, although the overall agreement remains very good.

Figure 2 shows the experimental $A(\omega)$ for a magnetic field along the [100] direction, along with the line-shape functions obtained from $\Gamma_2(\omega)$ and $\Gamma_4(\omega)$. The line-shape function obtained from Γ_4 is indistinguishable from the experimental curve, on the scale of the figure. This agreement is particularly satisfying since the experimental data for the [100] magnetic field have the least uncertainty. In contrast, the use of Γ_2 produces $\sim 10\%$ discrepancies and a spurious peak at $\omega\approx 1.2$. This peak may be understood

TABLE III. Values of the λ_n for $\Gamma_4(\omega)$.

	Crystallographic direction		
	[100]	[110]	[111]
Z	3.082 35	3.403 7	3.474 4
λ_2	0.151 26	0.082 987	0.086 966
λ_4	0.055 468	0.050 572	0.044 235

TABLE IV. Values of $A(\omega=0)$ obtained for the q-independent bubble model: exact results and two theoretical approximations.

N	From A_N	From Γ_N	Exact
2	1.26	1.13	1.14
4	1.26	1.13	1.14
8	1.16	1.14	1.14
12	1.17	1.14	1.14

as follows: $\Gamma_2(\omega)$ is a Gaussian approximation to the self-energy. The inclusion of additional moments flattens the peak of the Gaussian. $\Gamma_2(\omega)$ is therefore too large at $\omega=0$ and too small at larger ω, leading to a line-shape function which is too small at $\omega=0$ and having a peak at finite ω.

Figure 3 shows the time-dependent spin-correlation function[4] $G(t)$ for a magnetic field in the [100] direction. Along with the experimental curve, we display the Fourier transforms of $S_8(\omega)$ and the line-shape function obtained from $\Gamma_4(\omega)$. The best previous theoretical results for $A(\omega)$ were obtained[8] using A_4; our calculations show that $A_8(t)$ is practically indistinguishable from $A_4(t)$ on the scale of the figure. Both theoretical curves agree very well with the experimental curve on the scale of the inset. However, on the expanded scale it is clear that Γ_4 provides a much better description of $A(t)$ than does A_8: The height of the peak at $t\approx 5$ obtained from Γ_4 is within 10% of the experimental height, while that in A_8 is off by 50%. The depth of the trough at $t\approx 7$ obtained from Γ_4 is roughly $\frac{2}{3}$ of the experimental depth, while that in A_8 is less by a factor of $\frac{1}{6}$.

These results are at first surprising in view of the fact that Γ_4 uses as input only M_n with $n\leq 6$, while A_8 uses M_n with $n\leq 8$. However, we feel that the ME approximation is more appropriate for Γ than for A, for two reasons:

(1) The number of moment diagrams[6,9] contributing to Γ is smaller than that contributing to A. The frequency dependence of Γ is therefore expected to be smoother than that of A.

(2) The large-t behavior of $G(t)$ is expected to be dominated by a term proportional to $e^{-\alpha t}\cos(\beta t+\phi_0)$, arising from the singularity in $G(\omega)$ nearest to the real axis; α and β are determined by the position of the singularity, and ϕ_0 by the phase of its coefficient. The approximation

$$G(\omega)=\frac{i}{\omega-\Sigma_N(\omega)} \tag{11}$$

has poles off the real axis and can thus obtain the correct asymptotic behavior. By contrast, an approximate

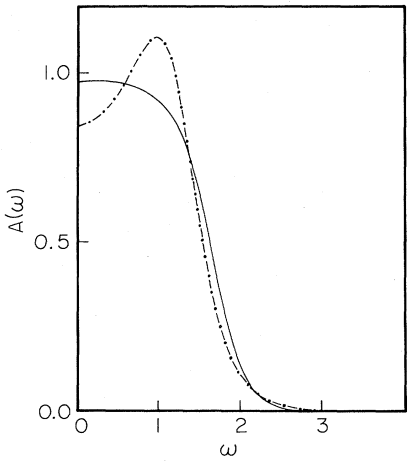

FIG. 2. Line-shape functions for magnetic field along the [100] direction. Solid line: experiment (Ref. 4) and theoretical values obtained from $\Gamma_4(\omega)$ [cf. Eq. (10)]. Dotted-dashed line: obtained from $\Gamma_2(\omega)$. Frequency measured in units of $(M_2)^{1/2}$.

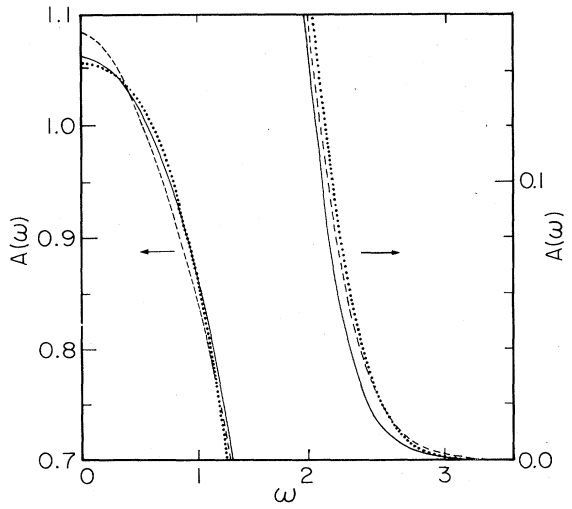

FIG. 1. Line-shape functions for magnetic field along the [110] direction. Solid line: experiment (Ref. 4). Dotted line: $A_8(\omega)$ [cf. Eq. (9)]. Dashed line: obtained from $\Gamma_4(\omega)$ [cf. Eq. (10)]. Frequency given in units of $(M_2)^{1/2}$.

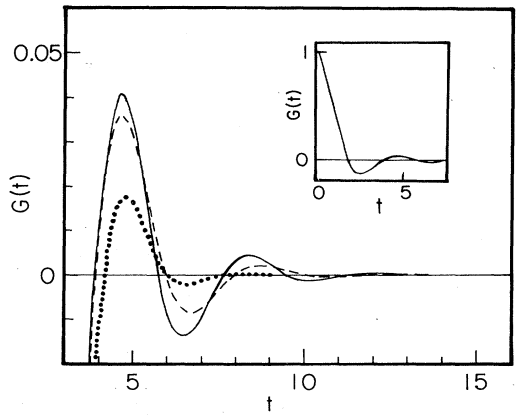

FIG. 3. Dynamical spin-correlation functions for magnetic field along the [100] direction. Solid line: experiment (Ref. 4). Dotted line: obtained from A_8 [cf. Eq. (9)]. Dashed line: obtained from Γ_4 [cf. Eq. (10)]. Time is given in units of $(M_2)^{-1/2}$.

Fourier transform of $A_N(\omega)$ using the method of stationary phase indicates an asymptotic behavior dominated by a term proportional to $e^{-\alpha t^{N/N-1}}$, rather than $e^{-\alpha t}$.

B. q-independent bubble

We have also performed ME fits to the correlation function in the q-independent bubble approximation described in Ref. 5. This is not a physically measurable function, but it is described exactly by the integral equation (in reduced units)

$$\Gamma(\omega)=\int \frac{d\omega'}{\pi} A(\omega')A(\omega-\omega') \ . \tag{12}$$

Further, high-order moments of this function can be easily calculated.[9] Thus it is a useful model for testing the method.

Our calculations support our beliefs about convergence that were discussed earlier. That is, $A_N(\omega)$ and $\Gamma_N(\omega)$ both converge only for $N=4k$ and not for $N=4k+2$. This was tested up to $N=12$. We believe that this alternating convergence property is connected with the absence of a sharp cutoff in $A(\omega)$ and $\Gamma(\omega)$. Both of these are believed to decay as $e^{-\alpha\omega}$ for some α. The ME approximations A_N and Γ_N, on the other hand, behave as $\exp(-\lambda_N\omega^N)$ for large ω. Thus for A_N and Γ_N to reproduce the $e^{-\alpha\omega}$ behavior over a large frequency interval, a large cancellation between the the high-order terms in the exponent is necessary. This requires the signs of the λ_n to alternate, which we believe is connected with the alternating convergence property. The alternation in the signs of the λ_n is seen explicitly in Table II. The necessity of the alternation is also apparent if one observes that expansion of the exponent $\alpha\omega$ in powers of ω^2 is equivalent to expansion of $\sqrt{x}$ in powers of $x-x_0$, where $x_0>0$; this expansion has alternating coefficients for any x_0.

As was seen earlier for the dipolar linewidth function, the fit to the exact function is demonstrably better when Γ_N is used as an intermediate step, rather than direct use of A_N. This is illustrated in Table IV, which displays the exact $A(\omega=0)$ along with the values obtained from A_N and Γ_N for $N\leq 12$. (The values for $N=2$ and 4 are identical because the ratios of the fourth moments to the squared second moments are such that $\lambda_4=0$ for both A_4 and Γ_4.) For $N\leq 4$, A_N differs from the exact value by over 10%, while the value obtained from Γ_N is already correct to within less than a percent. For $N=12$, the value obtained from Γ_N is essentially converged to the correct value, while A_N is still high by 3%.

III. CONCLUSION

The "unbiased" property of the extra information supplied by the ME method has previously provided greatly improved solutions for a number of missing information problems, ranging from image reconstruction to finite-temperature statistical mechanics.[1] The preceding analysis has demonstrated that the ME method provides an excellent description of the properties of high-temperature spin systems. We have also found same preliminary guidelines regarding the specific mode of application: much better results are obtained through the use of the self-energy operator as an intermediate step, instead of direct ME modeling of the line-shape function.

Future work in this field should extend the present analysis to obtain systematic criteria for the applicability of the method to problems of condensed-matter physics, and firm guidelines for the mode of application.

ACKNOWLEDGMENTS

We are grateful to Nick Papanicolaou and Lawrence Mead for allowing us to use their maximum-entropy code MAXENT. This work was supported in part by the National Science Foundation—Low Temperature Physics Program under Grant No. DMR-82-04166 and by the U.S. Department of Energy under Grant No. DE-FG02-84ER45130.

[1]See E. T. Jaynes, in *Papers on Probability, Statistics, and Statistical Physics,* edited by R. D. Rosenkrantz (Reidel, Dordrecht, Holland, 1983).

[2]Lawrence R. Mead and N. Papanicolaou, J. Math. Phys. **25**, 2404 (1984).

[3]See, for example, M. Engelsberg and I. J. Lowe, Phys. Rev. B **12**, 3547 (1975).

[4]M. Engelsberg and I. J. Lowe, Phys. Rev. B **10**, 822 (1974). The functional fits to $G(t)$ given in this reference were used to generate the exhibited values of $G(t)$. These fits were Fourier-transformed to obtain $A(\omega)$.

[5]S. J. Knak Jensen and E. Kjaersgaard Hansen, Phys. Rev. B **7**, 2910 (1973).

[6]C. W. Myles and P. A. Fedders, Phys. Rev. **9**, 4872 (1974).

[7]J. G. Powles and B. Carazza, in *Magnetic Resonance* (Plenum, New York, 1973), p. 133.

[8]G. W. Canters and C. S. Johnson, Jr., J. Magn. Reson. **6**, 1 (1972).

[9]C. Myles, Ph.D. thesis, Washington University, 1973 (unpublished).